

Compaction force in a confined granular column

D. Arroyo-Cetto, G. Pulos, R. Zenit,* and M. A. Jiménez-Zapata
*Instituto de Investigaciones en Materiales, Universidad Nacional Autónoma de México, Coyoacán,
 México Distrito Federal 04510, Mexico*

C. R. Wassgren

School of Mechanical Engineering, 585 Purdue Mall, Purdue University, West Lafayette, Indiana 47907-2088, USA

(Received 11 April 2003; published 7 November 2003)

Experiments to determine the force required to push a granular column confined within a cylinder were performed. The experimental apparatus was mounted on a material testing system machine in order to obtain force and displacement measurements simultaneously. Experiments were performed for two different sphere diameters, two different cylinder diameters and for a range of piston displacement velocities. The force necessary to displace the column increases rapidly with the column height, in accordance with Janssen's theory. More importantly, we found that this force also increases with the displacement velocity. This unexpected behavior is an indication of the transition to rate-dependent behavior in dense granular flows.

DOI: 10.1103/PhysRevE.68.051301

PACS number(s): 45.70.Cc, 46.55.+d, 81.05.Rm

Although granular materials have been the focus of many recent studies, a general consensus on how to accurately model their dynamics has not been reached. The primary obstacle to establishing a theoretical description of granular assemblies is that the behavior of an assembly can change significantly depending on a myriad of properties such as the local flow conditions, packing, surface roughness, temperature, and humidity. Repeating experimental results precisely is often a very difficult, sometimes impossible, task. There is a need for carefully controlled experiments to test some of the numerous existing theories.

We are, in particular, interested in understanding the transition from rate-independent [1–3] to rate-dependent behavior [4,5] in granular flows. The nature of the interactions between individual particles determines the overall mechanical behavior of the system. For enduring contacts, the behavior is dominated by friction and, hence, flow properties tend to be rate independent. However, when particles interact through collisions, inertial effects dominate and flow properties vary with the square of the shear rate. In most real flows, both types of contacts appear within the same flow domain [6]. The identification and proper description of the transition between these two flow limits is still an unresolved issue [4].

In this paper we investigate the forces generated by pushing a granular material through a cylinder. The stress distribution for a static granular bed in a cylindrical bin has been studied extensively [7]. The first model for predicting the static stresses in bin containing a granular material was given by Janssen *et al.* [8]. This simple model assumes that the radial (horizontal) stress σ_{rr} is proportional to the axial (vertical) stress σ_{zz} through a constant κ , i.e., $\sigma_{rr} = \kappa \sigma_{zz}$. Balancing vertical forces (material weight and the wall friction force) acting on a thin slice of the granular material gives

$$\frac{\partial \sigma_{zz}}{\partial z} + \frac{P}{A} \mu_w (\kappa \sigma_{zz}) = -\rho \nu g, \quad (1)$$

where P and A are the perimeter and cross-sectional area of the container, respectively. μ_w is the wall friction coefficient, ρ is the density of a single particle, and ν is the solid fraction. Despite its gross simplifications, Janssen's theory agrees well with experiments and is often used in silo design [7,9].

We present experimental results of the force required to push a granular column through a cylindrical container. This force is measured for two different particle and cylinder diameters over a wide range of column heights and displacement velocities. Rate-dependent behavior can be observed in this experiment even when the particle interactions are expected to be dominated by frictional, enduring contacts.

The experimental setup is shown schematically in Fig. 1, which consists of a cylinder-piston apparatus mounted on a material testing system (MTS) machine (model minibionics, 2.5 ton). The experimental arrangement holds the piston stationary while moving the cylinder downward [10]. The cylinder is moved at a constant velocity while the force acting on the piston base, referred to hereafter as the compaction force, is measured. A clearance of 0.25 mm between the cylinder and piston ensures that cylinder forces are not directly transmitted to the piston. Two piston diameters D of 25.4 and 50.8 mm were used in the experiments. The granular material consisted of nearly monodisperse glass spheres with diameters d of 3 and 6 mm (Jayco Co.). Cylinder velocities V_c ranged from 0.5 to 10 mm/s. The particles were poured into the cylinder with no particular care and all the experiments were carried out at room temperature and humidity levels. Similar experiments were conducted by [11–13]. In these previous experiments, very slow piston velocities were considered (less than 100 $\mu\text{m/s}$).

An experimental cycle consists of a compression period, during which the cylinder moves downward (in this period measurements are obtained). After the piston travels a preset distance, the experiment stops and the cylinder returns to its initial position at a constant velocity. The return motion causes the material to relax and expand back approximately to the same initial condition avoiding progressive compaction of the column. A few seconds later the experiment restarts. The cycle is repeated several times for each set of experimental conditions. Figure 2(a) shows typical experimental results for three different column heights ($H = 100$,

*Electronic address: zenit@servidor.unam.mx

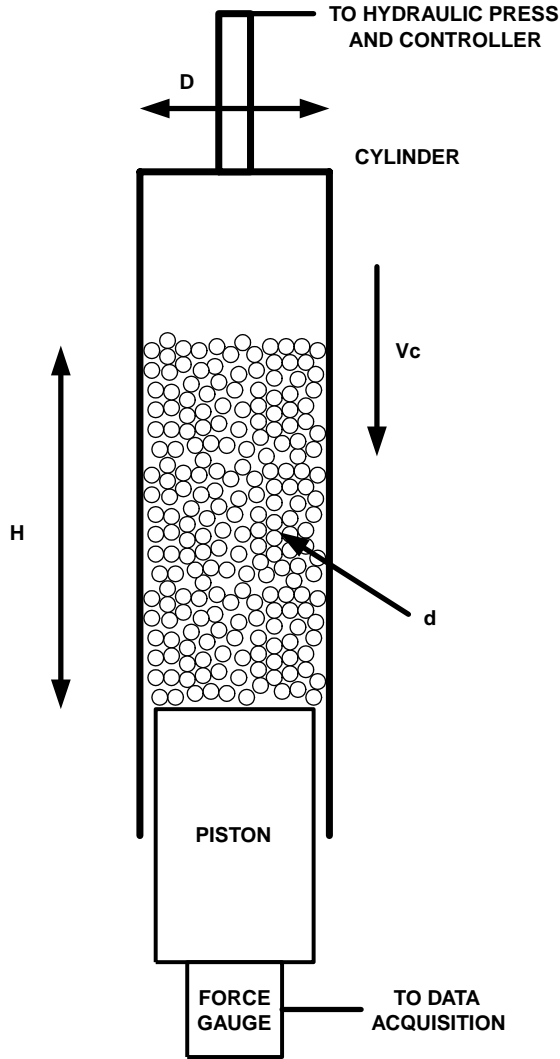


FIG. 1. A schematic of the experimental setup.

150, and 200 mm) using a fixed cylinder diameter ($D = 25.4$ mm), velocity ($V_c = 5$ mm/s), and particle diameter ($d = 3$ mm). The lines in the figure are the average of at least ten experiments. All the raw data from the experiments is shown to demonstrate the scatter in the measurements. In all the experiments the compaction force increases rapidly at the beginning of the experiment to an asymptotic mean value about which fluctuations occur. The force fluctuations do not show the saw-tooth structure observed at much smaller velocities [11,13].

Figure 2(b) shows the average of the force spectra from the experiments shown in Fig. 2(a). The spectra are shown as a function of the spatial frequency $f_\lambda = f/V_c$ (f is the frequency in 1/s and V_c is the cylinder speed in m/s, held constant for a given experiment). For spatial frequencies less than the particle scale ($1/d$), the power spectra decay at a rate close to f_λ^{-2} , which has been associated with stick-slip phenomena [14]. For frequencies larger than $1/d$, the decay is at a weaker rate for all cases. The increase in the overall magnitude of the spectra with increasing column height H indicates an increase in the magnitude of the force fluctuations.

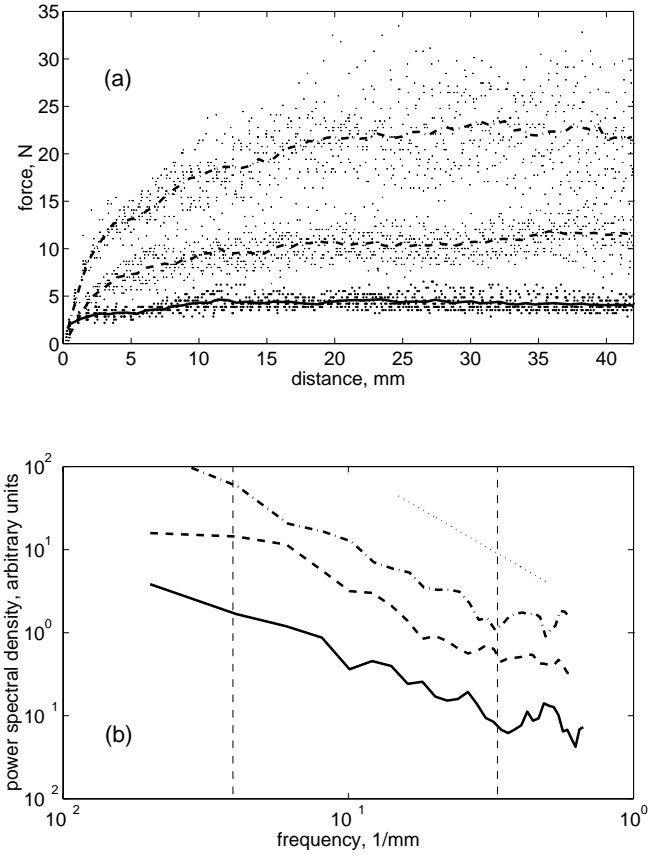


FIG. 2. (a) Compaction force as a function of cylinder displacement for three column heights H for a fixed cylinder diameter $D = 25.4$ mm, velocity $V_c = 5$ mm/s, and particle diameter $d = 3$ mm. The continuous line corresponds to $H = 100$ mm, the dashed line $H = 150$ mm, and the dash-dotted line $H = 200$ mm. The points around each line are the raw data from many experiments. (b) Average force power spectra as a function of spatial frequency for experiments in (a). The vertical dashed lines denote the characteristic spatial frequencies corresponding to $1/D$ and $1/d$. The straight dotted line shows a f_λ^{-2} decay.

The asymptotic compaction force in the experiment can be estimated using Janssen's theory, taking into account that the downward moving cylinder produces a friction force acting in the negative (upward) z direction. Solving Eq. (1) at the piston face ($z = H$), assuming a free surface at $z = 0$, and integrating over the area of the piston face, gives an expression for the compaction force, F_c :

$$F_c = \frac{\pi}{16} \frac{(D^*)^3 \rho v g}{\mu_w \kappa} \left[\exp\left(4 \mu_w \kappa \frac{H}{D^*}\right) - 1 \right], \quad (2)$$

where $D^* = D - d$ is an effective cylinder diameter that accounts for finite particle size effects. To compare the prediction from this model with the measurements, the value of the wall friction coefficient μ_w , and the proportionality constant κ must first be determined. The glass particles used in the experiments have a mass density of $\rho = 2500$ kg/m³. A solid fraction value of $\nu = 0.64$, corresponding to the maximum solid fraction, is assumed.

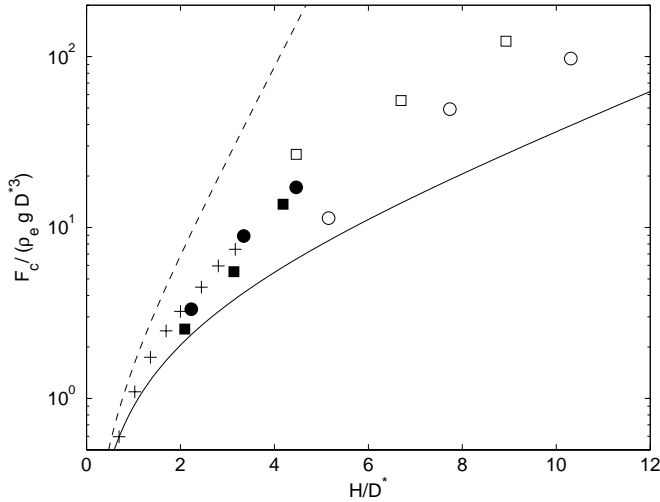


FIG. 3. Dimensionless mean asymptotic compaction force $F_c/(\rho_p g D^{*3})$ as a function of dimensionless column height H/D^* . The results are shown for a fixed value of the cylinder velocity $V_c=5$ mm/s. The squares and circles correspond to the 3 mm and 6 mm particles, respectively. The filled and empty symbols correspond to the results for 25.4 mm and 50.8 mm cylinder diameters, respectively. The plus signs are the data from Ref. [13].

A simple slider device was built to measure the wall friction coefficient μ_w . The device consisted of a flat surface, made of the same material as the cylinder, against which a plate of fixed glass particles was allowed to slide. Different weights were placed on the plate and the force required to pull the loaded plate at a constant velocity was measured. The friction coefficient, defined as the ratio of the tangential force to the normal load, was found to be a constant $\mu_w = 0.140 \pm 0.004$ over the range of velocities and loads corresponding to those in the compaction experiments. Other investigators have shown that, in fact, the instantaneous friction coefficient decreases during a ‘failure’ event of a plate sliding over a granular bed [15].

The value of κ can be determined once the internal friction coefficient is known, assuming wedge-type failure occurs [7]

$$\kappa = \frac{1 \mp \sin \phi}{1 \pm \sin \phi},$$

where ϕ is the internal friction angle of the material ($\phi = \tan^{-1} \mu_p$). Measurements of the material’s angle of repose indicate that $\phi = 22 \pm 1^\circ$. If the material fails actively (A), a negative sign is used in the numerator and a positive one in the denominator, and vice versa for a passive (P) failure. A value of $\phi = 22 \pm 1^\circ$ gives $\kappa_A = 0.45 \pm 0.02$ and $\kappa_P = 2.20 \pm 1.06$.

Figure 3 shows the dimensionless asymptotic compaction force $F_c/(\rho_p g D^{*3})$ as a function of the dimensionless column height H/D^* for all the cases tested with a piston velocity of $V_c=5$ mm/s. The exponential increase of the force with the column height is observed in all cases. In addition to the experimental measurements, the predictions using Eq. (2) are shown for both passive and active failure. As expected,

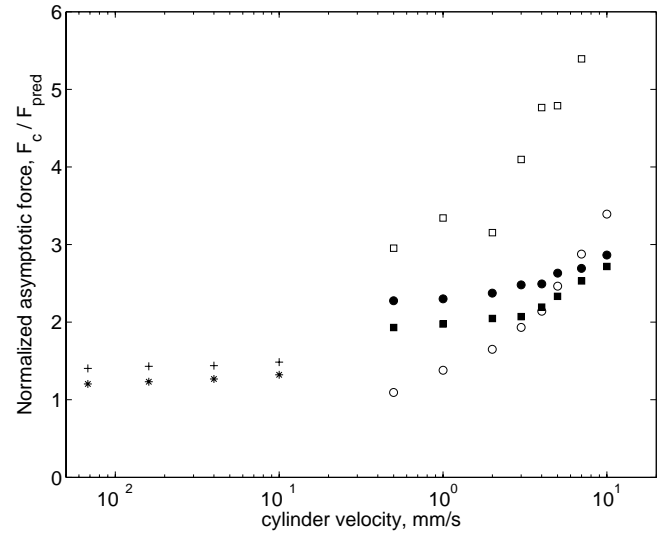


FIG. 4. Mean asymptotic compaction force as a function of the cylinder velocity in mm/s. The force is normalized by the static compaction force predicted by Eq. (2), considering an active failure mode. The results are shown for a fixed column height $H=200$ mm. The symbols are the same as in Fig. 2. The asterisks and plus signs are the data from Ref. [13] for relative humidities of <3% and 40%, respectively.

the measurements are bounded by the two failure limits. Data from the other tested piston velocities show similar trends with the results remaining bounded by the active and passive failure curves. The measurements of Ovarlez *et al.* [13] (also shown in the figure by the plus signs) are in good agreement with the present measurements despite the fact that Ovarlez *et al.* used shorter column heights and much smaller velocities.

The effect of cylinder velocity on the compaction force was also examined. For all the tested velocities, the compaction force behaves in a manner similar to that shown in Fig. 2. The force fluctuations do not vary significantly with increasing cylinder speed. However, the asymptotic compaction force increases with cylinder velocity for a given set of experimental conditions. Figure 4 plots the mean asymptotic force normalized by the static compaction force predicted by Eq. (2) as a function of the cylinder speed (in mm/s). The experimental data for two different cylinder and particle diameters are shown. The height of the column was maintained at $H=200$ mm in each of the experiments.

The asymptotic compaction force increases with increasing cylinder speed with the force being only weakly dependent on speed for small cylinder speeds and approaching a $\sqrt{V_c}$ dependence for larger speeds. The experimental measurements of Ovarlez *et al.* [13] are also shown in the figure for relative humidity values of 2% and 40%. The current experiments display a much stronger force-speed relationship than those obtained by Ovarlez *et al.* at much smaller velocities. They found a significant velocity-dependent force only for the cases in which the relative humidity level was high (greater than 50%).

We do not have a complete understanding of the measurements shown in Fig. 4. The direct measurement of the wall

friction coefficient was shown to be independent of the sliding velocity. One must bear in mind that the setup in which the measurement was obtained is different from that of the experiment; hence, the claim may not be entirely accurate. Other investigators have found that the friction coefficient shows a rich and complex behavior [15]. They found, however, that the friction coefficient may decrease during sliding of the granular material. This trend is opposite to that needed to explain our measurements. We consider that the increase in the compaction force cannot be attributed to a change in the particle/wall friction.

A plausible explanation of the observed trends can be formulated in terms of the compaction of the grain column during the experiment. Recently Campbell [16] reported a significant increase in the stress levels in dense sheared granular flows. An increase in the solid fraction of approximately 2% resulted in a stress magnitude increase of up to three orders of magnitude when the solid fraction is near the maximum packing limit. To validate this hypothesis, we performed a series of visualization experiments. We replaced the metal cylinder by a transparent lucite cylinder and measured the height before and after the compaction cycle for different cylinder speeds. A set of typical results is shown in Fig. 5. Clearly, the average density of the material increases as a function of the cylinder speed. Internal convection, observed both in the visualization experiments and in computer simulations [17], may also contribute to the compaction of the column. We believe that the material inside the column is going through a transition similar to that reported by Campbell. It is necessary to further investigate the magnitude of the convection cells inside the column. With an estimation of the average shear within the cylinder, it would be possible to evaluate the average shear in the column and further corroborate that, in fact, the shear causes compaction and an increase of the force.

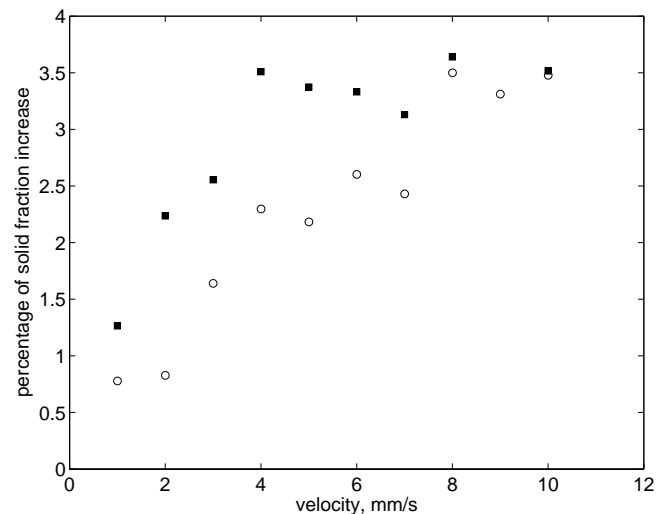


FIG. 5. Percentage of increase of the solid fraction $\Delta v/v_o \times 100$ as a function of the cylinder speed. The solid squares and the empty circles show results for $H=195$ mm and $H=130$ mm, respectively. For both cases $D=38.1$ mm and $d=6$ mm.

In summary, we report measurements of the compaction force in a confined granular column, which agree well with the predictions of Janssen's theory. Although the flow appears to have a majority of enduring particle contacts, the compaction force increases with the compaction speed. The rate at which the force increases also increases with increasing speed. We propose that the cause of the observed behavior results from a velocity-dependent compaction of the column.

The support of CONACYT (Grant No. NC-204) and UNAM-PAPIIT (Grant No. IN-110601) is greatly acknowledged.

-
- [1] R. Albert, M.A. Pfeifer, A.-L. Barabási, and P. Schiffer, *Phys. Rev. Lett.* **82**, 205 (1999).
- [2] K. Wieghardt, *Annu. Rev. Fluid Mech.* **7**, 89 (1975).
- [3] D. Chehata, R. Zenit, and C.R. Wassgren, *Phys. Fluids* **15**, 1622 (2003).
- [4] C.S. Campbell, *Annu. Rev. Fluid Mech.* **22**, 57 (1990).
- [5] C.R. Wassgren, R. Zenit, and A. Karion, *Phys. Fluids* **15**, 3318 (2003).
- [6] A.V. Potapov and C.S. Campbell, *Phys. Fluids* **8**, 2884 (1996).
- [7] R.M. Nedderman, *Statics and Kinematics of Granular Materials* (Cambridge University Press, Cambridge, 1992).
- [8] H.A. Janssen and Z. Vereins, *Deutsch Eng.* **39**, 1045 (1895).
- [9] P.G. de Gennes, *Physica A* **261**, 267–293 (1998).
- [10] If the cylinder moves at a constant velocity (no acceleration), the arrangement is equivalent to system in which the cylinder is kept fixed and the piston moves at the same constant velocity (Galilean transformation of nonaccelerating frames of reference).
- [11] E. Kolb, T. Mazozi, E. Clement, and J. Duran, *Eur. Phys. J. B* **8**, 483 (1999).
- [12] E. Vanel and E. Clement, *Eur. Phys. J. B* **11**, 525 (1999).
- [13] G. Ovarlez, E. Kolb, and E. Clement, *Phys. Rev. E* **64**, 060302 (2001).
- [14] B. Miller, C. O'Hern, and R.P. Behringer, *Phys. Rev. Lett.* **77**, 3110 (1996); A.L. Demirel and S. Granick, *ibid.* **77**, 4330 (1996); H.J.S. Feder and J. Feder, *ibid.* **66**, 2669 (1991).
- [15] S. Nasuno, A. Kudrolli, and J.P. Gollub, *Phys. Rev. Lett.* **79**, 949 (1997); S. Nasuno, A. Kudrolli, A. Bak, and J.P. Gollub, *Phys. Rev. E* **58**, 2161 (1998); F. Lacombe, S. Zapperi, and H.J. Herrmann, *Eur. Phys. J. E* **2**, 181 (2000).
- [16] C.S. Campbell, *J. Fluid Mech.* **465**, 261 (2002).
- [17] J. Lee, *J. Phys. A: Mat. Gen.* **27**, L257 (1994); C.R. Wassgren, Ph. D. thesis, California Institute of Technology, 1996.